Article

Molecular Cell

Interaction between AIF and CHCHD4 Regulates Respiratory Chain Biogenesis

Graphical Abstract

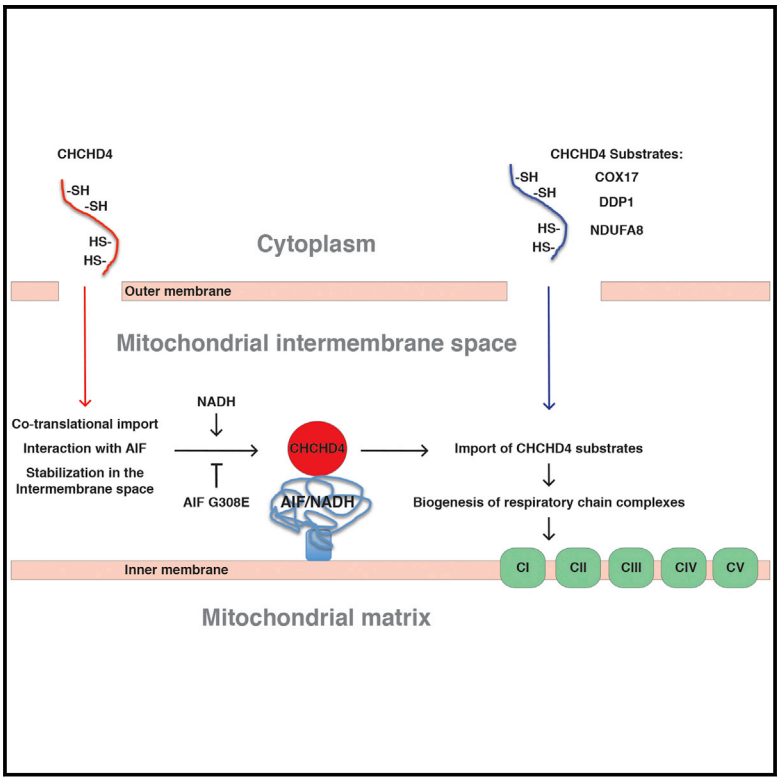

Highlights

- AIF interacts with CHCHD4, a regulator of the intermembrane space import machinery
- AIF regulates specific respiratory chain complexes by acting upstream of CHCHD4
- AIF is indispensable for translation-coupled mitochondrial import of CHCHD4
- Restoring CHCHD4 reverses the metabolic and cell death phenotypes of *Aif*$^{-/y}$ ESCs

Authors

Emilie Hangen, Olivier Féraud, Sylvie Lachkar, ..., Klas Blomgren, Guido Kroemer, Nazanine Modjtahedi

Correspondence

kroemer@orange.fr (G.K.), nazanine.modjtahedi@gustaveroussy.fr (N.M.)

In Brief

Hangen et al. show that the mitochondrial protein AIF regulates the biogenesis of respiratory chain complexes by interacting with, and by controlling the mitochondrial import of the mammalian homolog of yeast MIA40, CHCHD4, which is the central component of a redox-sensitive mitochondrial intermembrane space import machinery.

Hangen et al., 2015, Molecular Cell *58*, 1001–1014
June 18, 2015
http://dx.doi.org/10.1016/j.molcel.2015.04.020

Molecular Cell
Article

Interaction between AIF and CHCHD4 Regulates Respiratory Chain Biogenesis

Emilie Hangen,[1,2,3,4,5] Olivier Féraud,[6,7,8] Sylvie Lachkar,[1,2,3,4,5] Haiwei Mou,[1,2,3,4,5] Nunzianna Doti,[9] Gian Maria Fimia,[10,11] Ngoc-vy Lam,[1,2,3,4,5] Changlian Zhu,[12] Isabelle Godin,[3,6,13] Kevin Muller,[1,2,3,4,5] Afroditi Chatzi,[14,15] Esther Nuebel,[14,15] Fabiola Ciccosanti,[10] Stéphane Flamant,[6,7] Paule Bénit,[16,17] Jean-Luc Perfettini,[3,6,18,19] Allan Sauvat,[1,2,3,20] Annelise Bennaceur-Griscelli,[6,7,8,21] Karine Ser-Le Roux,[3,6,22] Patrick Gonin,[3,6,22] Kostas Tokatlidis,[14,15] Pierre Rustin,[16,17] Mauro Piacentini,[10,23] Menotti Ruvo,[9] Klas Blomgren,[12,24,25] Guido Kroemer,[1,2,3,4,5,20,26,27,*] and Nazanine Modjtahedi[1,2,3,4,5,27,*]

[1]Equipe 11 labellisée par la Ligue Nationale contre le Cancer, Centre de Recherche des Cordeliers, 75006 Paris, France
[2]INSERM, UMRS 1138, 75006 Paris, France
[3]Gustave Roussy Comprehensive Cancer Center, 94805 Villejuif, France
[4]Université Paris Descartes/Paris V, Sorbonne Paris Cité, 75006 Paris, France
[5]Université Pierre et Marie Curie, 75006 Paris, France
[6]Université Paris Sud/Paris XI, 94270 Kremlin Bicêtre, France
[7]INSERM U935, 94805 Villejuif, France
[8]ESTeam Paris Sud, Stem Cell Core Facility, Institut André Lwoff, 94800 Villejuif, France
[9]Istituto di Biostrutture e Bioimmagini, CNR, 80134 Napoli, Italy
[10]Department of Epidemiology and Preclinical Research, National Institute for Infectious Diseases IRCCS "L. Spallanzani," 00149 Rome, Italy
[11]Department of Biological and Environmental Sciences and Technologies (DiSTeBA), University of Salento, Lecce 73100, Italy
[12]Center for Brain Repair and Rehabilitation, Institute of Neuroscience and Physiology, University of Gothenburg, 40530 Gothenburg, Sweden
[13]INSERM U1009, 94805 Villejuif, France
[14]Institute of Molecular Cell and Systems Biology, University of Glasgow, G12 8QQ Glasgow, UK
[15]Institute of Molecular Biology and Biotechnology, Foundation for Research and Technology, Heraklion Crete 70013, Greece
[16]INSERM UMR1141, Hôpital Robert Debré, 75019 Paris, France
[17]Faculté de Médecine Denis Diderot, Université Paris 7, 75013 Paris, France
[18]Cell Death and Aging Team, Gustave Roussy, 94805 Villejuif, France
[19]INSERM U1030, Gustave Roussy, 94805 Villejuif, France
[20]Cell Biology and Metabolomics Platforms, Gustave Roussy Comprehensive Cancer Center, 94805 Villejuif, France
[21]Laboratoire d'Hématologie, Hôpital Paul Brousse AP-HP, 94800 Villejuif, France
[22]Animal and Veterinary Resources, 94805 Villejuif, France
[23]Department of Biology, University of Rome "Tor Vergata," 00133 Rome, Italy
[24]Department of Pediatrics, University of Gothenburg, The Queen Silvia Children's Hospital, 40530 Gothenburg, Sweden
[25]Karolinska Institute, Department of Women's and Children's Health, Karolinska University Hospital, 171 76 Stockholm, Sweden
[26]Pôle de Biologie, Hôpital Européen Georges Pompidou, AP-HP, 75015 Paris, France
[27]Co-senior author
*Correspondence: kroemer@orange.fr (G.K.), nazanine.modjtahedi@gustaveroussy.fr (N.M.)
http://dx.doi.org/10.1016/j.molcel.2015.04.020

SUMMARY

Apoptosis-inducing factor (AIF) is a mitochondrial flavoprotein that, beyond its apoptotic function, is required for the normal expression of major respiratory chain complexes. Here we identified an AIF-interacting protein, CHCHD4, which is the central component of a redox-sensitive mitochondrial intermembrane space import machinery. Depletion or hypomorphic mutation of AIF caused a downregulation of CHCHD4 protein by diminishing its mitochondrial import. CHCHD4 depletion sufficed to induce a respiratory defect that mimicked that observed in AIF-deficient cells. CHCHD4 levels could be restored in AIF-deficient cells by enforcing its AIF-independent mitochondrial localization. This modified CHCHD4 protein reestablished respiratory function in AIF-deficient cells and enabled AIF-deficient embryoid bodies to undergo cavitation, a process of programmed cell death required for embryonic morphogenesis. These findings explain how AIF contributes to the biogenesis of respiratory chain complexes, and they establish an unexpected link between the vital function of AIF and the propensity of cells to undergo apoptosis.

INTRODUCTION

Apoptosis-inducing factor (AIF) was initially characterized as a membrane-bound redox-active flavoprotein that is confined to the mitochondrial intermembrane space (IMS) of healthy cells, yet translocates to the nucleus upon the apoptosis-associated induction of mitochondrial outer membrane permeabilization (MOMP) (Susin et al., 1999) coupled to its proteolysis by calpains (Norberg et al., 2010). AIF has been involved in the execution of apoptosis throughout eukaryote phylogeny, in

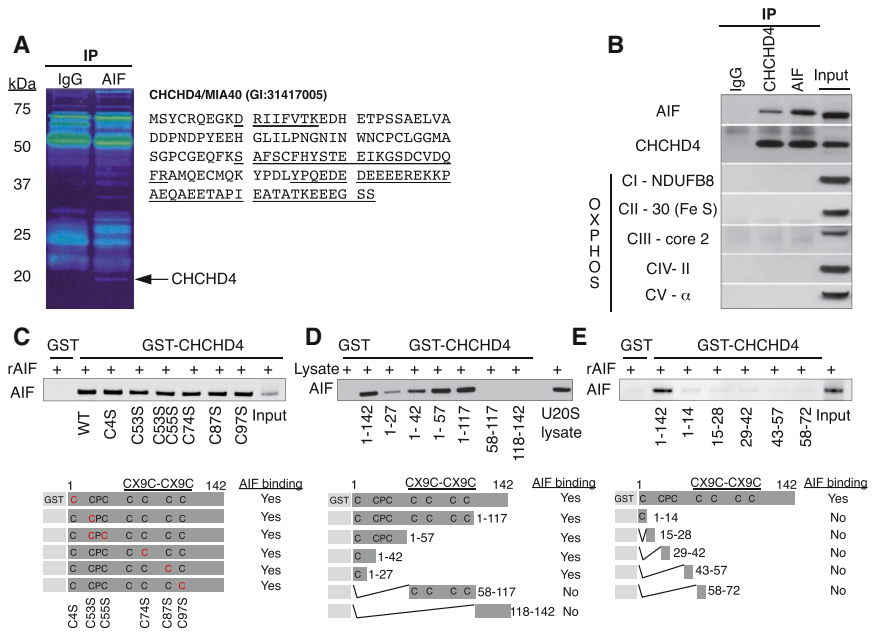

Figure 1. Physical Interaction between AIF and CHCHD4

(A) Identification of CHCHD4/MIA40 as an AIF-binding protein by immunoprecipitation of AIF (or as a control an isotype-matched rabbit IgG). Mass spectrometry-identified peptides that match CHCHD4 are underlined.

(B) Co-immunoprecipitation of AIF and CHCHD4 as performed on human cancer cell lysates. The presence of the indicated protein in the immune complex was checked by immunoblot. Whole-cell extract represents 25% of the input.

(C–E) Interaction of recombinant CHCHD4 with AIF. (C) Interaction of GST-tagged cysteine point mutants of CHCHD4 with recombinant AIF (rAIF) is shown. (D and E) Interactions of GST-tagged full-length and truncation mutants of CHCHD4 either with AIF contained in the U2OS cells lysate (D) or with rAIF (E) are shown. The indicated CHCHD4 derivatives (schematic presentations at bottom) were immobilized on beads and then evaluated for their capacity to bind AIF. Experiments were performed at least three times, yielding similar results. See also Figure S1.

yeast, filamentous fungi, nematodes, flies, and mammals (Hangen et al., 2010a; Joza et al., 2001). In the cytosol, AIF can signal for phosphatidylserine exposure on the plasma membrane (Susin et al., 1999). Moreover, in the nucleus, AIF can participate in chromatin condensation and caspase-independent large-scale DNA fragmentation (Susin et al., 1999), likely through direct electrostatic interaction with the DNA (Maté et al., 2002; Ye et al., 2002), as well as with other proteins that possess latent DNase activities (Parrish and Xue, 2003). AIF-deficient cells are resistant against a restricted panel of cell death inducers. In particular, mouse embryonic stem cells (ESCs) lacking AIF due to homologous recombination (*Aif*$^{-/y}$) fail to undergo cavitation (Feraud et al., 2007; Joza et al., 2001; Qi et al., 2012), which involves the first wave of programmed cell death during ontogeny.

Beyond its role in apoptosis, AIF participates in normal mitochondrial metabolism. In all species investigated, the absence of AIF causes a respiratory chain defect that is coupled to the post-transcriptional downregulation of protein subunits belonging to respiratory chain complexes I, III, and IV (Brown et al., 2006; Bénit et al., 2008; Hangen et al., 2010a; Pospisilik et al., 2007; Vahsen et al., 2004). Mice affected by a hypomorphic AIF mutation (Harlequin mice) or bearing tissue-specific knockout of AIF similarly develop severe neuromuscular mitochondriopathies leading to premature death (Klein et al., 2002; Hangen et al., 2010a). In humans, mutations in AIF manifest as familial X-linked diseases that have either of two different phenotypes. First, AIF mutations can cause a severe pediatric mitochondriopathy linked to reduced expression and function of respiratory chain complexes (Berger et al., 2011; Ghezzi et al., 2010). Second, the so-called Cowchock syndrome is caused by a mutation of AIF that increases its cytocidal potential (Rinaldi et al., 2012).

The relationship among AIF, respiratory function, and cavitation is elusive. Here we report the discovery of an AIF-interacting protein, CHCHD4, which provides a mechanistic link among AIF deficiency, mitochondrial dysfunction, and failed cavitation in ESCs.

RESULTS

AIF Interacts with CHCHD4

Immunoprecipitation of AIF from human cervical cancer cells followed by mass spectrometric sequencing of peptides led to the identification of CHCHD4.1, the human equivalent of yeast Mia40 (Tim40) (Chacinska et al., 2004; Naoé et al., 2004) as an AIF-binding partner (Figures 1A, 1B, and S1A). Human CHCHD4 is a soluble 16-kDa protein that localizes to the mitochondrial IMS (Hofmann et al., 2005), where it participates in mitochondrial import and catalyzes oxidative protein folding in cooperation with the sulfhydryl oxidase GFER/ALR/Erv1p (Banci et al., 2009; Chacinska et al., 2008; Fischer et al., 2013; Koch and Schmid, 2014). Endogenous AIF and CHCHD4, which both co-localized in mitochondria (Figure S1B), formed a stable complex that persisted even after the treatment of the cells with the translation inhibitor cycloheximide (CHX) (Figure S1C), and co-immunoprecipitated in conditions in which neither respiratory chain subunits nor GFER were detectable in the complex (Figure 1B; data not shown). Protein pull-down experiments revealed direct interaction of recombinant AIF with CHCHD4. This direct protein-protein interaction was not affected by point mutations of cysteine residues in CHCHD4 (Figure 1C) that previously have been implicated in its mitochondrial activity (Banci et al., 2009; Fraga et al., 2014; Hofmann et al., 2005; Koch and Schmid, 2014).

A subsequent scan of deletion mutants excluded the participation of the redox-active CX9C-CX9C domain of CHCHD4 in the interaction with AIF (Figures 1D and 1E). Rather, the N-terminal 27 amino acids of CHCHD4 (p1-27N-CHCHD4) were sufficient to interact with AIF (Figures 1D and 1E), and a

27-amino-acid synthetic peptide corresponding to this N terminus competitively disrupted the interaction of recombinant CHCHD4 with AIF (Figure S1D). While the interaction site of CHCHD4 could be precisely mapped to its N terminus, the interaction site of AIF appeared to be conformational. Accordingly, deletion of different domains of AIF resulted in the generation of a protein that failed to interact with CHCHD4, and only full-length AIF bound to CHCHD4 in cells (Figures S1E and S1F) as well as in GST pull-down experiments (Figure S1G). A pathogenic AIF mutation (E493V) that enhances its apoptotic activity (but does not affect its respiratory activity) (Rinaldi et al., 2012) did not alter the interaction with CHCHD4. In contrast, a mutant AIF, which carries a point mutation (G308E) in the binding domain to nicotinamide adenosine dinucleotide (NAD) and causes a severe complex I+IV deficiency (Berger et al., 2011; Ye et al., 2002), exhibited reduced CHCHD4 binding (Figures S1E and 2E). The addition of reduced pyrimidine nucleotides (NADH or NADPH), but not that of their oxidized equivalents (NAD^+ or $NADP^+$), favored the interaction between AIF and full-length CHCHD4 (Figures 2A and S2A–S2G), as well as that of AIF and the N-terminal fragment of CHCHD4, p1-27N-CHCHD4 (Figure 2B).

Isothermal titration calorimetry (ITC) confirmed the binding of p1-27N-CHCHD4 to AIF in a 1:1 stoichiometry in the presence of NADH (Figure 2C). NADH failed to affect the structure of p1-27N-CHCHD4 in conditions in which it altered that of AIF (Churbanova and Sevrioukova, 2008), as determined by far-UV circular dichroism (CD) (Figure 2D). NADH did affect the structure of the complex formed by p1-27N-CHCHD4 and AIF, as indicated by subtraction of the CD profiles obtained for the mixture of p1-27N-CHCHD4 plus AIF and the one obtained for AIF, in the absence or presence of NADH (Figure 2D). These results support the notion that the AIF-NADH complex possesses an increased capacity to bind CHCHD4 in comparison with AIF alone and that NADH levels stabilize the interaction between AIF and CHCHD4. Yet another argument in favor of this interpretation could be obtained with the aforementioned pathogenic AIF mutant (G308E), which affects the NADH-binding domain of AIF (Figures S1E and 2E). In GST pull-down assays involving non-mutated AIF protein immobilized to glutathione-sepharose beads and soluble CHCHD4 protein, the addition of NADH favored the interaction between both recombinant proteins (Figures 2A and 2F). However, the interaction between mutated G308E AIF protein and CHCHD4 was reduced at the basal level and was scarcely enhanced by the addition of NADH (Figure 2F).

Altogether, these results reveal the existence of the mitochondrial interactor of AIF, CHCHD4, which directly binds to the NADH-AIF complex via its N-terminal domain.

CHCHD4 Is Required for Respiratory Chain Biogenesis

Human CHCHD4 and its yeast ortholog MIA40 are involved in the import and assembly of mitochondrial IMS proteins (Banci et al., 2009; Chacinska et al., 2004, 2008; Naoé et al., 2004), which then impinge on the assembly and function of the respiratory chain (Allen et al., 2005; Bihlmaier et al., 2007; Chacinska et al., 2004; Dabir et al., 2007). To address the possibility that CHCHD4 might affect respiratory chain complexes in mammals, we created mice in which *Chchd4* was inactivated by mutational insertion to express a β-galactosidase-neo (β-GEO) reporter protein under the control of the *Chchd4* promoter (Figure 3A). Heterozygous expression of β-GEO was compatible with normal embryogenesis, revealing ubiquitous expression of the β-GEO transgene throughout development (Figure 3B). Intercrosses of heterozygous mice for homozygous disruption of the *Chchd4* locus yielded no $Chchd4^{-/-}$ pups at birth. No $Chchd4^{-/-}$ embryos were ever detected after embryonic day (E) E8.5 (Figure 3C). $Chchd4^{-/-}$ embryos were always staged at E5.5–6 (retarded embryos in Figure 3C), indicating that *Chchd4* deletion causes a developmental arrest coupled with embryonic lethality at the onset of gastrulation. The developmental retardation of $Chchd4^{-/-}$ embryos was accompanied by a major defect in the expression of respiratory chain complex I subunit CI-20 (Figure 3D).

In accord with this observation, we found that knockdown of CHCHD4 using two distinct small interfering RNAs (siRNAs) led to a similar respiratory chain defect in human osteosarcoma U2OS cells (Figure 4A). Thus, CHCHD4 depletion resulted in reduced protein expression of several respiratory chain subunits, such as CI-20 and CIV-II, paralleling functional defects in complexes I and IV, but not in complex V (Figures 4A–4E). As a control, depletion of Mic19, a homolog and potential interactor of CHCHD4 (Darshi et al., 2012; Pfanner et al., 2014), which does not co-immunoprecipitate with the AIF/CHCHD4 complex (Figure S3A), failed to mediate similar effects on the stability of the analyzed respiratory chain subunits (Figure S3B).

Taken together, these findings indicate that CHCHD4 plays a central role in the biogenesis of specific respiratory chain complexes.

AIF Is Required for CHCHD4 Protein Expression

The knockdown of CHCHD4 did not diminish the abundance of AIF (Figure 4A). In contrast, depletion of AIF led to a reduction of CHCHD4 protein expression (Figures 4A and 4F), yet failed to alter the levels of the related Mic19 protein (Figure S3B). The reduction of CHCHD4 protein in AIF-depleted cells was not accompanied by any change in the levels of CHCHD4 mRNA (Figure 4G). The biochemical and functional consequences of AIF depletion phenocopied that of CHCHD4 depletion, causing selective defects of respiratory chain complexes I and IV (Figures 4A–4E). Moreover, the knockdown of AIF or CHCHD4 had similar effects on the abundance of CHCHD4 substrates (Figures S3C–S3E) NDUFA8 (Szklarczyk et al., 2011), COX17, and DDP1 (Hofmann et al., 2005), which were not detectable in the AIF/CHCHD4 immunoprecipitate (Figure S3F), presumably because the interaction between CHCHD4 and its substrates is rather transient (Koch and Schmid, 2014; Sideris et al., 2009). Neither AIF nor CHCHD4 affected the abundance of other mitochondrial proteins such as VDAC, PINK, and HSP60 (Figures S3C and S3D). The mitochondrial IMS-operating metalloprotease YME1L (Baker et al., 2012; Jensen and Jasper, 2014) is (one of) the protease(s) that participates in the degradation of CHCHD4 substrates after depletion of AIF. Indeed, if the siRNA-mediated knockdown of AIF was accompanied by the simultaneous siRNA-mediated knockdown of YME1L, the depletion of CHCHD4 substrates such as COX17 (the copper chaperone for complex CIV) and NDUFA8 (Szklarczyk et al., 2011)

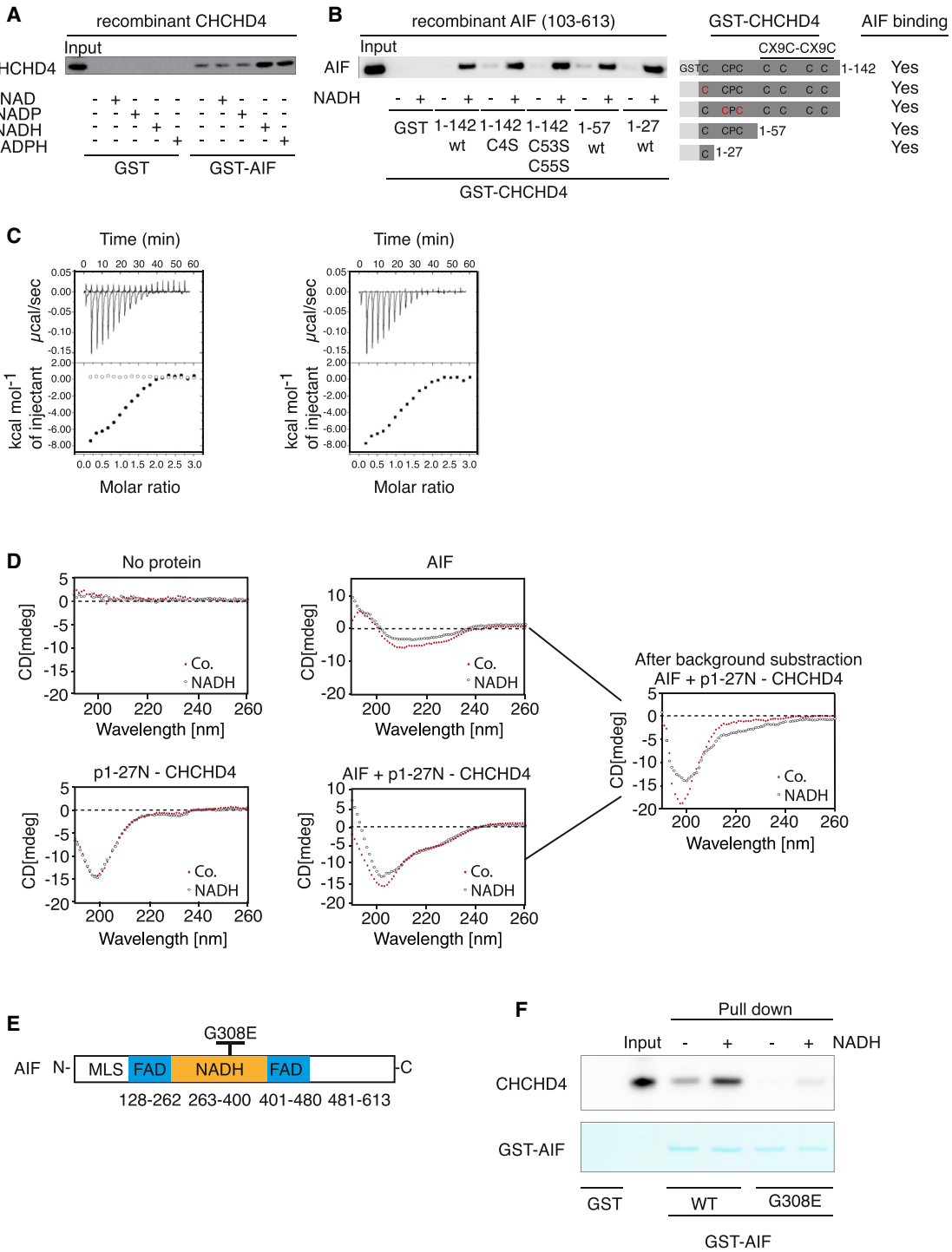

Figure 2. Impact of NADH on the Stabilization of AIF/CHCHD4 Complex

(A) Interaction of GST-tagged AIF with recombinant CHCHD4 (rCHCHD4) in the presence of pyrimidine nucleotides. GST-tagged AIF (103-613) was immobilized on beads, pre-incubated (+) or not (–) with pyrimidine nucleotides (NAD, NADP, NADH, and NADPH), and then evaluated for its capacity to bind rCHCHD4. Experiments were performed at least three times, yielding similar results.

(B) Interaction of GST-tagged mutants of CHCHD4 with AIF/NADH. The indicated WT or mutant GST-tagged CHCHD4 proteins (schematic presentation at right) were immobilized on beads and evaluated for their capacity to bind recombinant AIF (103-613) pre-complexed (+) or not (–) with NADH. All experiments were performed at least three times, yielding similar results.

(legend continued on next page)

(an IMS-localized subunit of complex CI required for the stabilization of the complex) was attenuated (Figure S3E).

AIF depletion by several non-overlapping siRNAs failed to affect the mitochondrial transmembrane potential (Joza et al., 2001; Figure S4C), yet caused a reduction of CHCHD4 protein expression with a delay of several days (Figures 5A, 5B, and S4D). Re-introduction of AIF expression by means of non-interferable plasmid constructs suppressed the effects of an AIF-specific siRNA on CHCHD4 expression (Figures S4A and S4B). These experiments revealed that both long isoforms of AIF, AIF1 and AIF2 (Hangen et al., 2010b), indistinguishably supported the expression of CHCHD4. Mice carrying the hypomorphic *Aif*$^{hq/y}$ mutation (i.e., male mice from the Harlequin strain), which develop signs of neurodegeneration at the adult stage, manifested a progressive CHCHD4 defect in the brain postpartum. This CHCHD4 defect preceded that of complex I subunits during early adulthood, as detected by quantitative immunoblots (Figures 5C, 5D, and S4E). The *Aif*$^{hq/y}$-associated defect in CHCHD4 protein expression occurred solely at the post-transcriptional level and was observed also in other organs from *Aif*$^{hq/y}$ mice (Figures S4F–S4H). AIF-deficient (*Aif*$^{-/y}$) ESCs also manifested reduced CHCHD4 expression compared to wild-type (WT) controls (Figures 5E and 5F).

Altogether, these findings suggest that AIF acts upstream of CHCHD4 to ensure optimal mitochondrial function at the level of selected protein complexes and that, in the absence of AIF, CHCHD4 substrates are unstable and destroyed by proteases such as YME1L.

AIF Controls the Mitochondrial Import of CHCHD4

As shown, AIF is required for the expression of CHCHD4 protein. AIF depletion had no effect on the half-life of CHCHD4 after translation blockade with CHX, excluding that the absence of AIF enhances the degradation of CHCHD4 (Figure S5A). Therefore, we investigated the potential effect of AIF on CHCHD4 import by creating an assay system. U2OS cells were transfected with a plasmid coding for the *Escherichia coli* biotin ligase BirA (de Boer et al., 2003) targeted to the mitochondrial IMS by means of a mitochondrial localization sequence (MLS) derived from the first 120 N-terminal residues of AIF (Otera et al., 2005). This plasmid was dubbed MLS-BirA. Simultaneously, cells were co-transfected with a CHCHD4 fusion construct (CHCHD4-b) that carried in its C terminus a biotin-accepting peptide for site-specific biotinylation by BirA (Figure 6A). MLS-BirA was exclusively detected in mitochondria (Figure 6C) facing the IMS (data not shown) and effectively biotinylated CHCHD4-b in a translation-dependent (CHX-repressible) manner (Figure 6B). Knockdown of AIF reduced the biotinylation of CHCHD4-b as it reduced the overall abundance of CHCHD4-b (Figure 6D). Thus, knockdown of AIF negatively affected the expression of endogenous CHCHD4, the overall protein levels of CHCHD4-b, as well as those of biotinylated CHCHD4-b, to a similar level (Figure S5B), in line with the interpretation that the translation-dependent biotinylation of CHCHD4-b by MLS-BirA reflects its overall abundance. Kinetic experiments, during which biotin was removed from culture media before CHX treatment and the translation was restarted by CHX removal in the presence of biotin, confirmed that AIF depletion (by means of two distinct siRNAs) reduced the rate of CHCHD4-b biotinylation (Figures 6E and S5C).

Next, we explored the putative implication of AIF in translation-coupled import by measuring co-translation within a fusion construct composed by N-terminal CHCHD4 and C-terminal unstable GFP (Li et al., 1998), which were separated by the 2A self-cleaving peptide (de Felipe et al., 2006; Figure 6F). The 2A self-cleaving peptide provokes ribosomal skipping, causing an apparent cleavage at this site without the need of proteolysis (de Felipe et al., 2006). We transfected this new construct into cells and observed that the co-translation of both recombinant CHCHD4 (upstream of 2A) and GFP (downstream of 2A) was attenuated when AIF was depleted. This effect was quantified in two ways, namely by assessing the GFP-dependent fluorescence of cells (by flow cytometry) and by measuring the expression of GFP by immunoblot, yielding concordant results (Figures 6F–6I). Hence, by interfering with the co-translational import of CHCHD4 into mitochondria, AIF depletion also reduced the translation of GFP in this system. In contrast, AIF depletion failed to affect the translation of another, co-transfected control plasmid (MLS-BirA) that also codes for a mitochondrial protein, underscoring the specificity of the effects. Altogether, this assay corroborates the hypothesis that AIF controls the translation-coupled mitochondrial import of CHCHD4.

(C) ITC profiles of AIF interaction with the synthetic peptide p1-27N-CHCHD4 in the presence of NADH. (Top left) Raw data for sequential injections of a p1-27N-CHCHD4 solution into PBS (supplemented with NADH) used as blank and hAIF(Δ1-103) solution (supplemented with NADH) are shown. (Bottom left) Plot shows the heat evolved (kilocalories) per mole of p1-27N-CHCHD4 added to the buffer solution (open circle) and into the hAIF(Δ1-103) solution (filled circle). (Right) Titration of hAIF(Δ1-103) with p1-27N-CHCHD4, corrected for the heat of p1-27N-CHCHD4 dilution, against the molar ratio of p1-27N-CHCHD4 to hAIF(Δ1-103) is shown. The data were fitted to a single-site binding model. Plots are representative of at least three independent determinations.

(D) Secondary structure analysis of p1-27N-CHCHD4/hAIF(Δ1-103) interaction using far-UV CD in the absence (filled circle, Co.) or presence (open circle, NADH) of NADH is shown. (Top left) CD spectra were collected on the buffer alone. (Bottom left) CD spectra were collected on the p1-27N-CHCHD4 solution. Addition of the flavonoid does not induce any structural change on the peptide. (Top middle) CD spectra were collected on the hAIF(Δ1-103) solution. As expected, the presence of NADH largely influences the structure of the protein. (Bottom middle) CD spectra were recorded on the combined p1-27N-CHCHD4 and hAIF(Δ1-103) solution. (Right) The same spectra shown at bottom middle after subtraction of the hAIF(Δ1-103) contribution presented at top middle are shown. The peptide undergoes a large conformational rearrangement due to the interaction with the protein, but the conformational change is larger in the presence of the cofactor. Spectra are representative of at least three independent determinations.

(E) Schematic localization of G308E mutation in the NADH-binding domain of AIF is shown.

(F) Pull-down of GST-tagged WT AIF or mutated AIF^{G308E} with the His-tagged CHCHD4 protein, in the presence or absence of NADH. GST-tagged AIF (103-613) WT or mutated G308E were immobilized on beads, pre-incubated (+) or not (–) with NADH, and then evaluated for their capacity to bind rCHCHD4. The immunoblot (top) was realized using the indicated antibody. The membrane was stained with a blue protein stain for GST-AIF loading control (bottom). Experiments were performed at least three times, yielding similar results.

See also Figure S2.

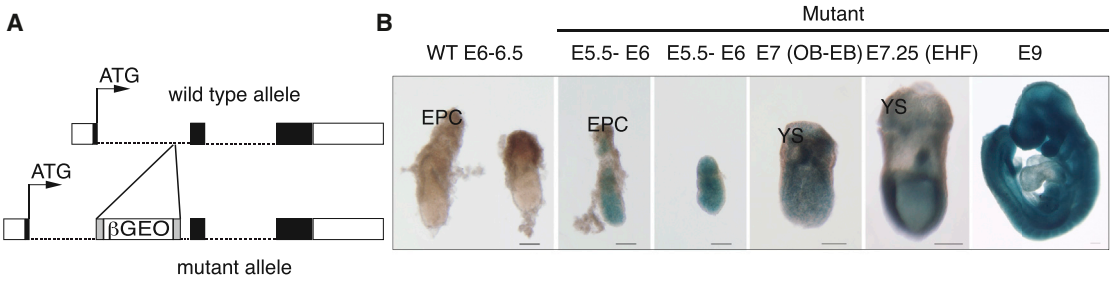

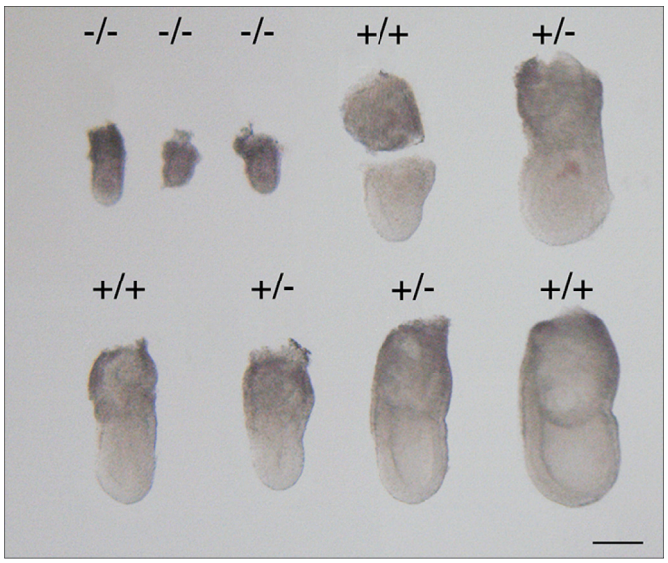

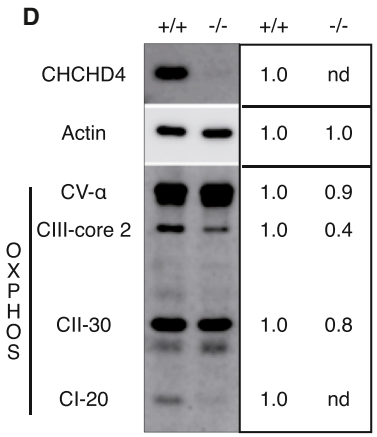

Parameters	Days post-fertilization	
	7.5 - 8.5	**9.5 - 10**
N° of embryos (litters)	164 (21)	39 (6)
% *CHCHD4* $^{+/+}$	21.1	22.6
% *CHCHD4* $^{+/-}$	61.2	77.4
% *CHCHD4* $^{-/-}$	17.6	0

Parameters	Days post-fertilization	
	7 - 7.5	**8 - 8.5**
N° of embryos (litters)	86 (10)	49 (6)
Retarded embryos with *CHCHD4* $^{+/+}$ genotype	0	0
Retarded embryos with *CHCHD4* $^{+/-}$ genotype	10/86	2/49
Retarded embryos with *CHCHD4* $^{-/-}$ genotype	18/86	10/49

Figure 3. Impact of CHCHD4 Knockout on Respiratory Chain Complexes during Embryogenesis

(A) Schematic representation of the gene trap strategy used for the insertional mutagenesis of *CHCHD4* gene. The insertion of the βGEO cassette, at the vicinity of exon 2, disrupts the endogenous coding sequence and allows the expression of a β-galactosidase-neo reporter mRNA that is initiated in the first exon of *CHCHD4* and reports the transcriptional activity of the locus.

(B) X-Gal staining of mutant embryos from E5.5 to E9 revealed a widespread expression of CHCHD4, with the exception of the visceral endoderm at the earliest stages. EPC, ectoplacental cone; YS, yolk sac. Scale bars, 200 μM.

(legend continued on next page)

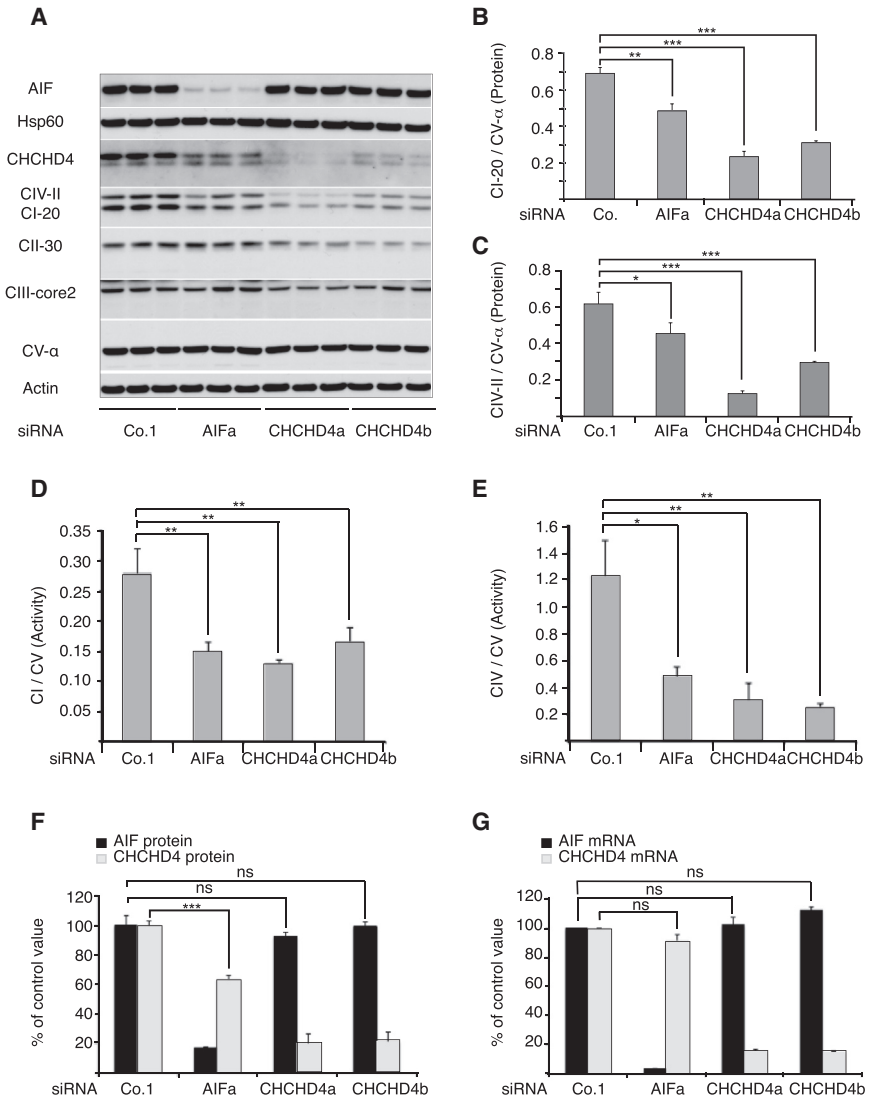

Figure 4. Impact of AIF and CHCHD4 Depletion on the Levels of Mitochondrial Proteins

(A) U2OS cell extracts (triplicates), subjected to the transfection with siRNAs that deplete AIF (AIFa), CHCHD4 (CHCHD4a, CHCHD4b), or Emerin as a control (Co.1), were analyzed by immunoblot for the abundance of the indicated proteins (A).

(B, C, and F) The relative expression levels of proteins (with respect to complex V subunit CV-α) were quantified by image analysis (B, C, and F). In (F), the ratio of AIF or CHCHD4 protein to CV-α is set to 100% in control siRNA-transfected cells.

(D and E) The relative deficiency of complex I and IV activity (with respect to complex V) was analyzed by spectrophotometric measurement of individual respiratory chain complexes activities.

(G) Relative AIF or CHCHD4 mRNA levels were determined by qRT-PCR, defining the ratio of AIF or CHCHD4 to three housekeeping mRNAs in control siRNA-transfected cells set to 100%. Values are means ± SEM of triplicates. *$p < 0.05$, **$p < 0.01$, ***$p < 0.001$ calculated by ordinary one-way ANOVA followed by Bonferroni's post-analyses.

See also Figure S3.

affected by one of the AIF-specific siRNAs (AIFc), yet was strongly reduced by another siRNA (AIFa) that targets the stretch of the mRNA sequence corresponding to the MLS shared by AIF and MC (Figures 7B and S6B). Importantly, MC was able to revert the defects in DDP1 and respiratory chain complex subunits (CI-20 and GRIM 19 from complex I, CIV-II from complex IV, and the CIV-chaperone COX17) secondary to AIF depletion (Figures 7B and S6B). In contrast, a control construct (MB, composed of the same MLS from AIF and an irrelevant protein, BirA) was unable to reverse the respiratory chain subunit defect induced by AIF depletion (Figure 7B). Mutation of all functional cysteines contained in CHCHD4 abrogated the capacity of the MC construct to restore the mitochondrial defects of AIF-deficient cells (Figure S6C), underscoring the relevance of the cysteine-dependent oxidoreductase activity of CHCHD4.

Enforced Mitochondrial CHCHD4 Import Restores Respiration in AIF-Deficient Cells

The absence of AIF was incompatible with enforced high expression of HA-tagged CHCHD4 protein (Figure S6A). For this reason, we attempted to restore the expression of CHCHD4 in AIF-depleted cells by modifying its mitochondrial import pathway and enforcing its attachment to the inner membrane, with a MLS derived from the first 120 N-terminal residues of AIF (Otera et al., 2005) fused to its N terminus (Figure 7A). The expression level of this MLS-CHCHD4 chimera (MC) was not

Stable transfection with MC, but not with MB, could also restore the expression of CI-20 in undifferentiated *Aif*$^{-/y}$ ESCs, as well as in *Aif*$^{-/y}$ embryoid bodies (EBs) that are formed from ESCs upon depletion of leukemia-inhibitor factor (LIF), a

(C) CHCHD4 invalidation leads to embryonic lethality at gastrulation. Embryos indicated as retarded embryos were staged at E5.5–6. In addition to homozygous (*CHCHD4*$^{-/-}$) embryos that were nearly always staged at E5.5–6, some heterozygous embryos (*CHCHD4*$^{+/-}$) staged at E5.5–6 also were recovered from the litters containing homozygous knockout embryos (bottom table). Scale bar, 200 μM.

(D) Impact of *CHCHD4* mutation on the expression of respiratory chain complexes protein subunits. Extracts of individual embryos, staged at E5.5–6, were analyzed by immunoblot (left). The abundance of indicated proteins in the mutant embryo (−/−, deficient for the expression of CHCHD4) was quantified by image analysis and normalized compared to the levels of same proteins in the embryo proficient for the expression of CHCHD4 (+/+) (right). Actin was used as a loading control. Nd, not detectable.

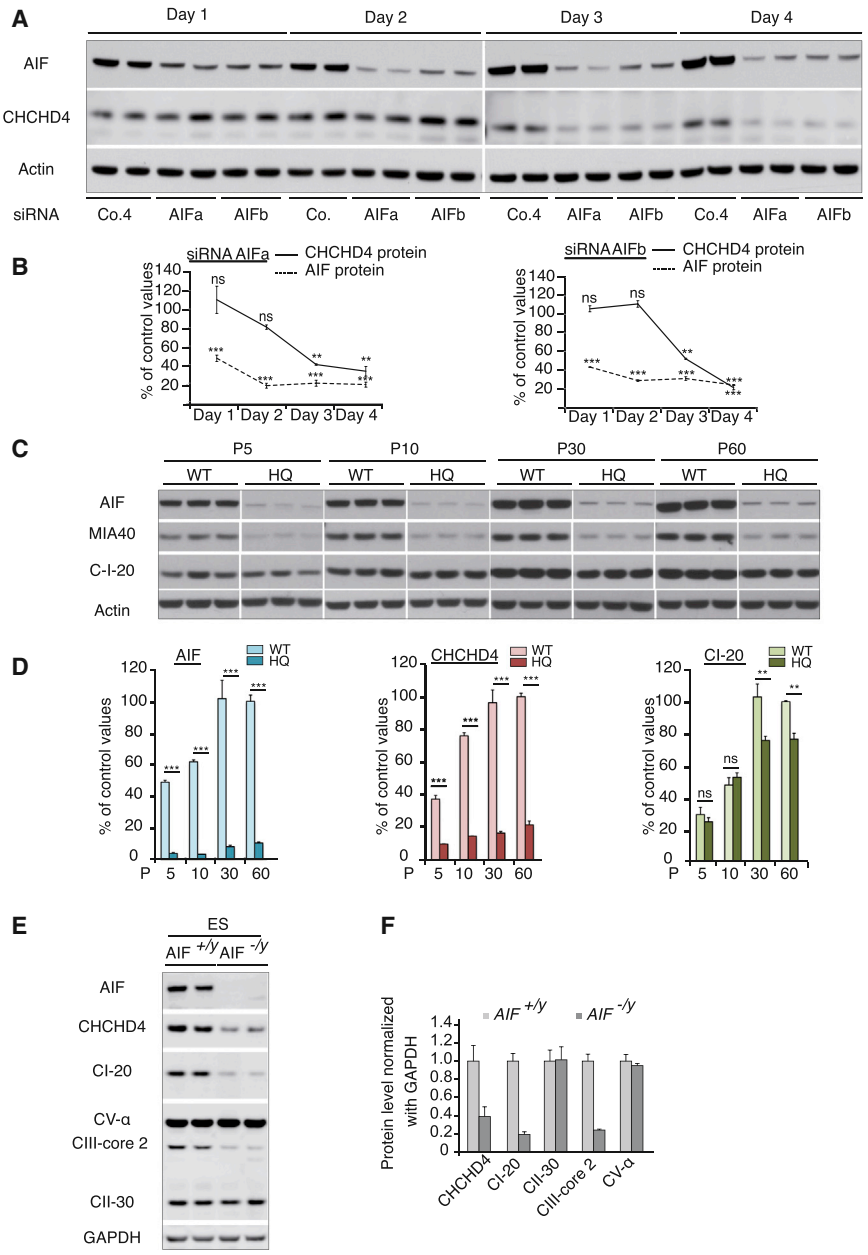

Figure 5. Kinetic Ordering of the AIF/CHCHD4 Pathway

(A and B) Extracts of U2OS cells, transfected with the indicated siRNAs for 1 to 4 days, were analyzed by immunoblot (A), and the relative abundance of AIF and CHCHD4 was quantified by image analysis followed by normalization compared to actin levels (B). Results were expressed as a percentage of control value (siRNA Co.4) defined as 100%. Values are means ± SD of duplicates. *p < 0.05, **p < 0.01, ***p < 0.001 calculated by ANOVA followed by Bonferroni's post-analyses.

(C and D) The kinetic impact of the HQ mutation on AIF, CHCHD4, and complex-I-20 protein expression was determined in brain samples collected at the indicated day postpartum. Triplicate samples from WT (*Aif*$^{+/y}$) and mutant (*Aif*$^{hq/y}$) mice were analyzed by immunoblot (C), and the relative abundance of each protein was determined by quantitative image analysis followed by normalization compared to actin levels. Results were expressed as a percentage of control value, with P60-WT defined as 100% (D). Values are means ± SEM of triplicates. *p < 0.05, **p < 0.01, ***p < 0.001 calculated by ANOVA followed by Bonferroni's post-analyses.

(E and F) Mouse ESC lines AIF WT (*Aif*$^{+/Y}$, two independent cell lines) and AIF deficient (*Aif*$^{-/Y}$, two independent cell lines) were analyzed by immunoblot for the abundance of the indicated proteins (E), and the relative expression levels of proteins were quantified by image analysis and normalized compared to the level of GAPDH (F). See also Figure S4.

cytokine that usually maintains the pluripotency and represses the differentiation of ESCs (Murray and Edgar, 2001). This effect was obtained both in normoxic (Figures 7C and 7D) and hypoxic (Figures S6D and S6E) conditions. Concomitantly, MC, but not MB, improved the function of respiratory chain complexes I and IV in *Aif*$^{-/y}$ ESCs (Figure 7E) and restored the capacity of the cells to form cavitating EBs upon LIF removal. MC-expressing *Aif*$^{-/y}$ EBs underwent cavitation in conditions in which MB-expressing or untransfected (not shown) *Aif*$^{-/y}$ EBs failed to undergo cavitation (Figures 7F and 7G). In contrast, MC had no impact on the formation and size of EBs (Figure 7G).

Altogether, these results indicate that restoring CHCHD4 levels can reverse the phenotype of *Aif*$^{-/y}$ ESCs with respect to their metabolic and cell death phenotypes.

DISCUSSION

As shown here, there are several lines of evidence that place CHCHD4 in the pathway linking AIF deficiency to the deficient biogenesis of respiratory chain complexes. First, there is chronological evidence. In Harlequin mice, which bear a retroviral insertion in the first intron of AIF, causing a reduction of its expression, the defect in CHCHD4 becomes evident before a major reduction of respiratory chain complex I is detectable at the postnatal stage. Second, there is functional evidence in favor of a mechanistic hierarchy between AIF and CHCHD4. Depletion or deletion of AIF causes a reduction in the abundance of CHCHD4. Conversely, knockdown of CHCHD4 fails to affect the expression of AIF. Hence, AIF is required for CHCHD4 expression, not vice versa. Third, the depletion of either AIF or CHCHD4 causes similar defects in a specific set of mitochondrial proteins, including components of the respiratory chain complexes I and IV and DDP1. Fourth, when the import of CHCHD4 into the mitochondrial IMS is rendered independent from AIF, namely by fusing the MLS of AIF with CHCHD4, the resulting chimeric protein MC is able to overcome the respiratory chain defect that is normally detectable in AIF-depleted cells. This

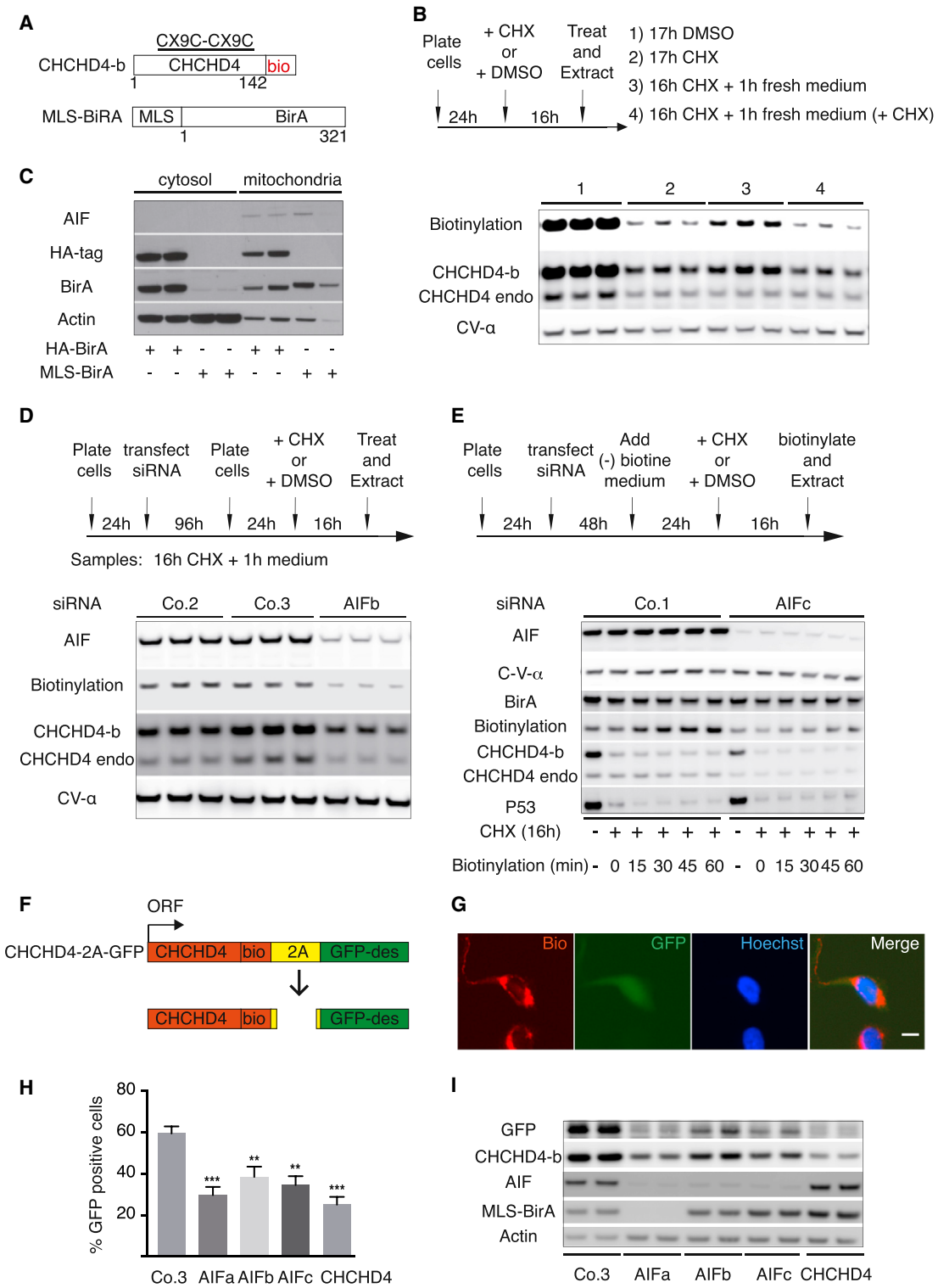

Figure 6. Regulation of CHCHD4 Translation/Import by AIF

(A) Schematic representations show the biotinable CHCHD4-b that carries in its C terminus an acceptor peptide (GLNDIFEAQ(**K**)IEWHE) flanking a lysine residue that is specifically biotinylated by BirA and MLS-BirA, the mitochondrion-targeted BirA, which is addressed to the organelle by means of an MLS derived from the first 120 N-terminal residues of AIF.

(legend continued on next page)

experimental observation closes the cycle of argumentation. CHCHD4 depletion is indispensable for the phenotypic manifestation of an AIF-related defect in oxidative phosphorylation.

How does AIF affect the expression levels of CHCHD4? Having excluded the possibility that AIF might influence the levels of CHCHD4 mRNA, we evaluated the hypothesis that AIF would affect the import of CHCHD4 into mitochondria. To test this possibility, we determined the capacity of AIF to regulate the import of CHCHD4 protein in human cells. For this, we first created an experimental system in which a bacterial biotinylase specifically targeted to the IMS was combined with a biotinable CHCHD4 (CHCHD4-b), meaning that the degree of CHCHD4-b in vivo biotinylation reflects its localization to mitochondria. Kinetic experiments led to the conclusion that the import of CHCHD4 into mitochondria was translation-dependent (because it only occurred in the absence of CHX) and that it was affected by the abundance of AIF. In AIF-deficient cells, the biotinylation (and hence import) of CHCHD4-b by the IMS-targeted biotinylase was reduced. Second, we developed a protein co-translation assay in which unstable (non-mitochondrial) GFP was placed downstream of CHCHD4-b on the same mRNA, in the same open reading frame, finding that AIF deficiency reduced the abundance of GFP in conditions in which it affected CHCHD4-b expression. Translation-dependent import is not a rarity (Weis et al., 2013). However, to the best of our knowledge, this is the first report that AIF can affect such an import reaction.

How might the presence of AIF in mitochondria facilitate the translation-dependent import of CHCHD4? It appears plausible that AIF affects the import of CHCHD4 through a specific effect. Indeed, AIF was found to physically interact within cells with CHCHD4, and our results show that the AIF/CHCHD4 interaction is a direct one, not requiring additional proteins. No specific interaction domain within AIF could be identified by deletion scanning, suggesting that this interaction relies on the entire tertiary structure of the AIF protein. In line with this interpretation, we found that NADH (or NADPH) enhanced the binding of AIF to CHCHD4, knowing that only the holo-AIF protein (but none of the deletion mutants studied here) possesses NADH or NADPH reductase activity (Maté et al., 2002; Ye et al., 2002). Moreover, a mitochondriopathy-associated point mutation occurring within the NADH-binding domain of AIF (Berger et al., 2011) reduced the interaction with CHCHD4, and the addition of NADH barely ameliorated the formation of the complex. In contrast to AIF, the binding of CHCHD4 involved a short domain. The N-terminal, 27-amino-acid-long fragment of CHCHD4 was necessary and sufficient for it to interact with AIF, while the redox function of CHCHD4 was irrelevant to the CHCHD4/AIF interaction. The N terminus of CHCHD4 is unstructured when examined by nuclear magnetic resonance (NMR) spectroscopy (Banci et al., 2009). However, far-UV CD data and ITC profiles were compatible with the idea that this peptide firmly interacts with AIF, in particular in the presence of NADH. Future co-crystallization of these interactors may confirm the hypothesis that the N terminus of CHCHD4 acquires a defined structure as it binds to AIF. Irrespective of these incognita, it appears plausible that AIF may drag the CHCHD4 N terminus into the mitochondrial IMS, thereby facilitating its import. Once the entire CHCHD4 protein has been taken up into this compartment, it may adopt its mature conformation and catalyze oxidative protein folding by virtue of its capacity to form mixed disulfides with protein substrates (Milenkovic et al., 2009; Sideris et al., 2009), thereby contributing to optimal mitochondrial biogenesis (Yang et al., 2012). It is possible, but still remains to be determined, that CHCHD4 bound to AIF maintains its catalytic activity by transiently interacting with its partner enzyme (Erv1) and its substrates. Obviously, it will be interesting to investigate the possibility that CHCHD4

(B) Assessment of translation-coupled import of CHCHD4 in the mitochondrion. U2OS cells, stably overexpressing CHCHD4-b and MLS-BirA proteins, were incubated in the absence (DMSO) or presence of CHX for 16 hr (schematic protocol in the figure). Then, cells (3) and (4) were washed and re-incubated, only for 1 hr, in the absence (3) or presence (4) of CHX. Finally, the biotinylation of CHCHD4-b and the abundance of the indicated proteins were analyzed on triplicate samples and compared to that of control samples incubated for 17 hr in the absence (1, DMSO) or presence (2, CHX) of CHX.

(C) Mitochondrial localization of MLS-BirA. The subcellular localization of MLS-BirA was compared to that of an HA-tagged BirA by immunoblot analysis of the indicated proteins in the mitochondrial and cytosolic extracts.

(D) Impact of AIF knockdown on the translation-coupled import of CHCHD4 in the mitochondrion. U2OS cells stably overexpressing CHCHD4-b and MLS-BirA were transfected with control siRNAs (Co.2 and Co.3) or an AIF-specific siRNA (AIFb) and submitted to the CHX treatment protocol described in (B). Only extracts prepared from cells incubated in the presence of CHX for 16 hr and then washed and re-incubated for 1 hr in the absence of CHX (16 hr CHX + 1 hr fresh medium) are presented. The biotinylation of CHCHD4-b and the abundance of the indicated proteins in the lysates of AIF knockdown cells are analyzed on triplicate samples and compared to that of triplicate samples from cells transfected with control siRNA Co.2 and Co.3.

(E) Impact of AIF knockdown on the kinetics of the translation-coupled import of CHCHD4 into mitochondria. U2OS cells stably overexpressing the biotinable CHCHD4-b and MLS-BirA were transfected with control siRNAs (Co.1) or an AIF-specific siRNA (AIFc) and submitted to a successive biotin-deprivation and CHX-treatment protocol presented in the figure. Then, 16 hr after CHX treatment, cells were washed and incubated for the indicated times in the presence of fresh CHX-free medium supplemented with 8 μM biotin. Finally, extracts were analyzed for the biotinylation of CHCHD4 and levels of the indicated proteins.

(F–I) Impact of AIF knockdown on the translation-coupled expression of CHCHD4-b and GFP. (F) The construct CHCHD4-b-2A-GFP is designed to produce a single fusion ORF composed by an N-terminal CHCHD4 and a C-terminal unstable GFP protein (Li et al., 1998), which are linked to each other by a 2A self-cleaving peptide (de Felipe et al., 2006). (G) During the translation phase, the self-processing of the 2A peptide allows the production of CHCHD4-b that is imported into the mitochondrion and biotinylated by MLS-BirA, while the GFP protein is diffused everywhere in the cell. Biotinylated CHCHD4-b (Bio) is revealed by indirect immunofluorescence in the presence of phycoerythrin-coupled streptavidin. Scale bar, 10 μm. (H–I) U2OS cells stably co-transfected with CHCHD4-b-2A-GFP and MLS-BirA plasmids were transfected with control siRNA (Co.3), AIF-specific siRNAs (AIFa, AIFb, or AIFc), or with CHCHD4-specific siRNA (CHCHD4a). Four days post-transfection, the abundance of GFP in AIF knockdown cells is analyzed by fluorescence (flow cytometry) (H) or by immunoblot, in parallel to the indicated proteins (I) and compared to that of samples prepared with cells transfected with control Co.3 siRNA or CHCHD4 siRNA that knocks down directly the fusion RNA CHCHD4-b-2A-GFP. The graph (H) shows the percentage of GFP-positive cells observed after transfection with the indicated siRNA. Values are means ± SEM of five independent experiments. *$p < 0.05$, **$p < 0.01$, ***$p < 0.001$ calculated by ANOVA followed by Bonferroni's post-analyses. See also Figure S5.

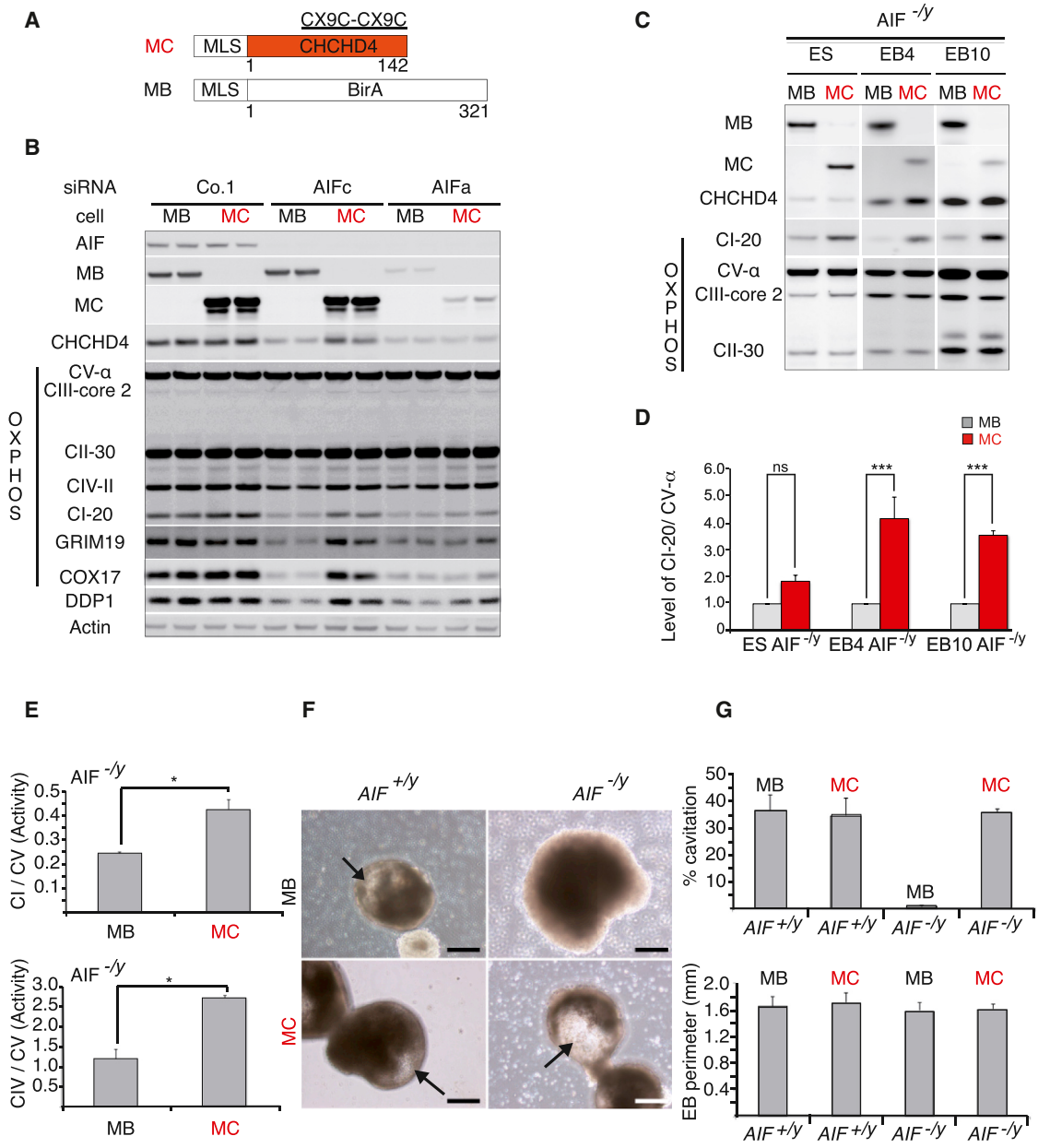

Figure 7. Phenotypic Reversal of the AIF Defect by Mitochondrion-Targeted CHCHD4

(A) Schematic representation shows the mitochondrion-targeted CHCHD4 (MC) and BirA (MB), which both share an identical MLS derived from the first 120 N-terminal residues of AIF.

(B) Impact of MC and MB on the abundance of mitochondrial proteins of AIF-depleted cells. U2OS cells were stably transfected with either MC or MB, and then subjected to the knockdown of Emerin (control, Co.1) or AIF, using either an siRNA that only targets AIF (AIFc) or another siRNA (AIFa) that targets both AIF and MC or MB (which all contain identical, AIF-derived N-termini). The abundance of the indicated proteins was determined by immunoblot.

(C and D) Impact of MC and MB on the abundance of mitochondrial proteins in AIF-null mutant cells. Mutant (*Aif*$^{-/y}$) murine cells were stably transfected with MC or MB and grown in the conditions of high oxygen tension (normoxia). Then, lysates were prepared from ESCs (grown in the presence of LIF) or EBs (EB4 and EB10 generated, respectively, by the withdrawal of LIF for 4 and 10 days) and analyzed for the expression of the transgene and respiratory chain-related proteins (C). The relative expression level of CI-20 subunit protein was quantified by image analysis and normalized compared to the level of CV-α protein subunit (D). Values are means ± SEM of at least three independent experiments. *$p < 0.05$, **$p < 0.01$, ***$p < 0.001$ calculated by one-way ANOVA followed by Bonferroni's post-analyses. Data are representative of at least three experiments that yielded comparable results.

(E) Histograms show the respiratory function of mutant (*Aif*$^{-/y}$) ESCs stably transfected with MC or MB. Values are means ± SEM of triplicates. *$p < 0.05$, **$p < 0.01$, ***$p < 0.001$ calculated by t test (with Welch's correction).

(F and G) Phenotype of EBs derived from WT (*Aif*$^{+/y}$) and mutant (*Aif*$^{-/y}$) ESCs stably transfected with MC or MB. Representative pictures are shown for EBs of the indicated genotype (bar, 200 μm) (F). Histograms show the percentage of cystic EBs (G, top) and the measure of their perimeter (G, bottom) is presented. See also Figure S6.

mutations could provoke similar phenotypes as those described for its interactors, AIF and Erv1 (Di Fonzo et al., 2009).

Unexpectedly, we found that the phenotype of AIF-null ($AIF^{-/y}$) ESCs with regard to cavitation (Feraud et al., 2007; Joza et al., 2001) was secondary to the mitochondrial dysfunction. Following up the finding that partial inhibition of the respiratory chain complex I with rotenone was sufficient to abolish cavitation in WT EB (Feraud et al., 2007), we observed that transfection of $AIF^{-/y}$ ESCs with mitochondrion-targeted CHCHD4, a maneuver that corrected the mitochondrial defect, also restored the capacity of $AIF^{-/y}$ ESCs to undergo cavitation upon in vitro differentiation. At present, the precise molecular mechanisms that link oxidative phosphorylation to cavitation-associated programmed cell death remain elusive.

Altogether, we conclude that the effect of AIF on the biogenesis of the mitochondrial respiratory chain complexes is mediated by its physical and functional interaction with CHCHD4, an essential mitochondrial intermembrane protein.

EXPERIMENTAL PROCEDURES

Animals

All procedures and animal experimentation protocols (project authorization 2012-076) were reviewed and deemed acceptable by Registered Ethical Committee 26, and carried out in the animal facility of Gustave Roussy (official agreement number E-94-076-11).

Cell Culture and Transfection

Human osteosarcoma U2OS cells (ATCC HTB-96) were cultured as described previously (Hangen et al., 2010b). Pools of transfected U2OS cells were established by co-transfection with plasmids described in the Supplemental Experimental Procedures followed by selection in 0.5 μg/ml puromycin (Invivogen) and 0.5 mg/ml geneticin (Life Technologies). Mouse ESC culture and manipulation protocols are described in the Supplemental Experimental Procedures.

Translation-Coupled Mitochondrial Import of CHCHD4

U2OS cells stably overexpressing the biotinable CHCHD4 (CHCHD4-b) and the mitochondrion-targeted BirA (MLS-BirA), transfected or not with siRNA, were incubated in the presence of the reversible protein translation inhibitor CHX for 16 hr. Then, for the purpose of reactivating protein translation, CHX was washed away using PBS and cells were re-incubated, only for 1 hr, in a fresh medium free of CHX. Finally, triplicate samples were extracted with 2×SB (4% SDS, 20% glycerol, 125 mM Tris-HCl (pH 6.8), and 200 mM DTT), boiled, resolved with SDS/PAGE (NUPAGE, Life Technologies), and analyzed by immunoblot. The kinetic of in vivo biotinylation of CHCHD4-b was assessed using the aforementioned protocol except that, 24 hr before the addition of CHX, the regular medium was replaced by a biotin-depleted one (prepared as described in the Supplemental Experimental Procedures). After 16 hr of CHX treatment (in the absence of biotin), cells were washed with PBS and incubated for 0 to 60 min with the biotin-depleted CHX-free medium supplemented with 8 μM biotin (Sigma-Aldrich). To assess the in vivo biotinylation of CHCHD4-b, after transferring the SDS-PAGE-separated proteins, the nitrocellulose membrane (Bio-Rad) was first blocked by incubation with 1% BSA diluted in TBST buffer (10 mM Tris-HCl (pH 8.0), 150 mM NaCl, and 0.05% Tween 20) for 1 hr and then incubated for a further 1 hr with a horseradish peroxidase-conjugated streptavidin (Sigma-Aldrich). Finally the biotin-streptavidin binding was detected with the enhanced chemiluminescence (ECL) detection kit (GE Healthcare).

Statistical Analyses

GraphPad Prism 5.0d software was used for statistical analyses. Groups were compared by one-way ANOVA followed by Bonferroni post-analyses or unpaired two-tailed t test with Welch's corrections. The criterion for statistical significance was set at $p < 0.05$. Data are expressed as mean ± SEM.

SUPPLEMENTAL INFORMATION

Supplemental Information includes Supplemental Experimental Procedures and six figures and can be found with this article online at http://dx.doi.org/10.1016/j.molcel.2015.04.020.

AUTHOR CONTRIBUTIONS

E.H., O.F., S.L., H.M., N.D., G.M.F., N.L., C.Z., I.G., K.M., A.C., E.N., F.C., S.F., P.B., A.S., P.R., K.S.-L., and N.M. performed experiments. E.H., O.F., N.D., G.M.F., I.G., A.C., J.-L.P., A.B.-G., P.G., K.T., A.S., P.R., M.P., M.R., K.B., G.K., and N.M. analyzed results. E.H., G.K., and N.M. prepared the figures. G.K. and N.M. designed the research and wrote the paper.

ACKNOWLEDGMENTS

We are grateful to Eric Jacquet (Imagif, France) for qRT-PCR analyses; Aurélie Sauvage, Mélanie Polrot, Benoît Petit, and Mirile Ganga for their help with animal experimentation; Josef M. Penninger for AIF knockout mouse ESCs; Denis Biard for Epstein-Barr virus-based episomal vector; and John Stroubolis for the gift of bacterial biotin ligase expression vector 3XHA-BiRA pBUDneo. This work was supported by Agence Nationale de Recherche (ANR). E.H. was supported by Ligue contre le Cancer, H.M. by ANR, S.F. by Région Ile-de-France (DIM STEM-Pôle). G.K. was supported by the Ligue contre le Cancer (équipe labelisée); Projets blancs; ANR under the frame of E-Rare-2, the ERA-Net for Research on Rare Diseases; Association pour la recherche sur le cancer (ARC); Cancéropôle Ile-de-France; Institut National du Cancer (INCa); Fondation Bettencourt-Schueller; Fondation de France; Fondation pour la Recherche Médicale (FRM); the European Commission (ArtForce); the European Research Council (ERC); the LabEx Immuno-Oncology; and the Paris Alliance of Cancer Research Institutes (PACRI). ESTeam Paris Sud was supported by the University Paris Sud. P.R. was supported by ANR and Association Française contre les Maladies Mitochondriales. C.Z. was supported by the Swedish Research Council, the Swedish Childhood Cancer Foundation, the Frimurare Barnhus Foundation, Swedish governmental grants to scientists working in health care, the Wilhelm and Martina Lundgren Foundation, and the National Nature Science Foundation of China. M.R. was supported by FIRB MERIT, project RBNE08NKH7_003. M.P. was supported by the Italian Ministry of University and Research (PRIN 2009/2011 and FIRB Accordi di Programma 2011) and EU grant "Transpath." M.P. and G.M.F. were supported by grants from the Italian Ministry of Health (Ricerca Finalizzata and Ricerca Corrente) and AIRC. J.-L.P. was supported by ANR and NATIXIS. K.T. was supported by the UK Royal Society, the Scottish Universities Life Science Association (SULSA), the Wellcome Trust (Institutional Strategic Support Funds), European Union (European Social Fund—ESF), and the Operational Program "Education and Lifelong Learning" of the National Strategic Reference Framework (NSRF): THALES and the Greek General Secretariat for Research and Technology Program ARISTEIA.

Received: September 15, 2014
Revised: February 27, 2015
Accepted: April 14, 2015
Published: May 21, 2015

REFERENCES

Allen, S., Balabanidou, V., Sideris, D.P., Lisowsky, T., and Tokatlidis, K. (2005). Erv1 mediates the Mia40-dependent protein import pathway and provides a functional link to the respiratory chain by shuttling electrons to cytochrome c. J. Mol. Biol. *353*, 937–944.

Baker, M.J., Mooga, V.P., Guiard, B., Langer, T., Ryan, M.T., and Stojanovski, D. (2012). Impaired folding of the mitochondrial small TIM chaperones induces clearance by the i-AAA protease. J. Mol. Biol. *424*, 227–239.

Banci, L., Bertini, I., Cefaro, C., Ciofi-Baffoni, S., Gallo, A., Martinelli, M., Sideris, D.P., Katrakili, N., and Tokatlidis, K. (2009). MIA40 is an oxidoreductase that

catalyzes oxidative protein folding in mitochondria. Nat. Struct. Mol. Biol. *16*, 198–206.

Bénit, P., Goncalves, S., Dassa, E.P., Brière, J.J., and Rustin, P. (2008). The variability of the harlequin mouse phenotype resembles that of human mitochondrial-complex I-deficiency syndromes. PLoS ONE *3*, e3208.

Berger, I., Ben-Neriah, Z., Dor-Wolman, T., Shaag, A., Saada, A., Zenvirt, S., Raas-Rothschild, A., Nadjari, M., Kaestner, K.H., and Elpeleg, O. (2011). Early prenatal ventriculomegaly due to an AIFM1 mutation identified by linkage analysis and whole exome sequencing. Mol. Genet. Metab. *104*, 517–520.

Bihlmaier, K., Mesecke, N., Terziyska, N., Bien, M., Hell, K., and Herrmann, J.M. (2007). The disulfide relay system of mitochondria is connected to the respiratory chain. J. Cell Biol. *179*, 389–395.

Brown, D., Yu, B.D., Joza, N., Bénit, P., Meneses, J., Firpo, M., Rustin, P., Penninger, J.M., and Martin, G.R. (2006). Loss of Aif function causes cell death in the mouse embryo, but the temporal progression of patterning is normal. Proc. Natl. Acad. Sci. USA *103*, 9918–9923.

Chacinska, A., Pfannschmidt, S., Wiedemann, N., Kozjak, V., Sanjuán Szklarz, L.K., Schulze-Specking, A., Truscott, K.N., Guiard, B., Meisinger, C., and Pfanner, N. (2004). Essential role of Mia40 in import and assembly of mitochondrial intermembrane space proteins. EMBO J. *23*, 3735–3746.

Chacinska, A., Guiard, B., Müller, J.M., Schulze-Specking, A., Gabriel, K., Kutik, S., and Pfanner, N. (2008). Mitochondrial biogenesis, switching the sorting pathway of the intermembrane space receptor Mia40. J. Biol. Chem. *283*, 29723–29729.

Churbanova, I.Y., and Sevrioukova, I.F. (2008). Redox-dependent changes in molecular properties of mitochondrial apoptosis-inducing factor. J. Biol. Chem. *283*, 5622–5631.

Dabir, D.V., Leverich, E.P., Kim, S.K., Tsai, F.D., Hirasawa, M., Knaff, D.B., and Koehler, C.M. (2007). A role for cytochrome c and cytochrome c peroxidase in electron shuttling from Erv1. EMBO J. *26*, 4801–4811.

Darshi, M., Trinh, K.N., Murphy, A.N., and Taylor, S.S. (2012). Targeting and import mechanism of coiled-coil helix coiled-coil helix domain-containing protein 3 (ChChd3) into the mitochondrial intermembrane space. J. Biol. Chem. *287*, 39480–39491.

de Boer, E., Rodriguez, P., Bonte, E., Krijgsveld, J., Katsantoni, E., Heck, A., Grosveld, F., and Strouboulis, J. (2003). Efficient biotinylation and single-step purification of tagged transcription factors in mammalian cells and transgenic mice. Proc. Natl. Acad. Sci. USA *100*, 7480–7485.

de Felipe, P., Luke, G.A., Hughes, L.E., Gani, D., Halpin, C., and Ryan, M.D. (2006). E unum pluribus: multiple proteins from a self-processing polyprotein. Trends Biotechnol. *24*, 68–75.

Di Fonzo, A., Ronchi, D., Lodi, T., Fassone, E., Tigano, M., Lamperti, C., Corti, S., Bordoni, A., Fortunato, F., Nizzardo, M., et al. (2009). The mitochondrial disulfide relay system protein GFER is mutated in autosomal-recessive myopathy with cataract and combined respiratory-chain deficiency. Am. J. Hum. Genet. *84*, 594–604.

Feraud, O., Debili, N., Penninger, J.M., and Kroemer, G. (2007). Cavitation of embryoid bodies requires optimal oxidative phosphorylation and AIF. Cell Death Differ. *14*, 385–387.

Fischer, M., Horn, S., Belkacemi, A., Kojer, K., Petrungaro, C., Habich, M., Ali, M., Küttner, V., Bien, M., Kauff, F., et al. (2013). Protein import and oxidative folding in the mitochondrial intermembrane space of intact mammalian cells. Mol. Biol. Cell *24*, 2160–2170.

Fraga, H., Bech-Serra, J.J., Canals, F., Ortega, G., Millet, O., and Ventura, S. (2014). The mitochondrial intermembrane space oxireductase Mia40 funnels the oxidative folding pathway of the cytochrome c oxidase assembly protein Cox19. J. Biol. Chem. *289*, 9852–9864.

Ghezzi, D., Sevrioukova, I., Invernizzi, F., Lamperti, C., Mora, M., D'Adamo, P., Novara, F., Zuffardi, O., Uziel, G., and Zeviani, M. (2010). Severe X-linked mitochondrial encephalomyopathy associated with a mutation in apoptosis-inducing factor. Am. J. Hum. Genet. *86*, 639–649.

Hangen, E., Blomgren, K., Bénit, P., Kroemer, G., and Modjtahedi, N. (2010a). Life with or without AIF. Trends Biochem. Sci. *35*, 278–287.

Hangen, E., De Zio, D., Bordi, M., Zhu, C., Dessen, P., Caffin, F., Lachkar, S., Perfettini, J.L., Lazar, V., Benard, J., et al. (2010b). A brain-specific isoform of mitochondrial apoptosis-inducing factor: AIF2. Cell Death Differ. *17*, 1155–1166.

Hofmann, S., Rothbauer, U., Mühlenbein, N., Baiker, K., Hell, K., and Bauer, M.F. (2005). Functional and mutational characterization of human MIA40 acting during import into the mitochondrial intermembrane space. J. Mol. Biol. *353*, 517–528.

Jensen, M.B., and Jasper, H. (2014). Mitochondrial proteostasis in the control of aging and longevity. Cell Metab. *20*, 214–225.

Joza, N., Susin, S.A., Daugas, E., Stanford, W.L., Cho, S.K., Li, C.Y., Sasaki, T., Elia, A.J., Cheng, H.Y., Ravagnan, L., et al. (2001). Essential role of the mitochondrial apoptosis-inducing factor in programmed cell death. Nature *410*, 549–554.

Klein, J.A., Longo-Guess, C.M., Rossmann, M.P., Seburn, K.L., Hurd, R.E., Frankel, W.N., Bronson, R.T., and Ackerman, S.L. (2002). The harlequin mouse mutation downregulates apoptosis-inducing factor. Nature *419*, 367–374.

Koch, J.R., and Schmid, F.X. (2014). Mia40 targets cysteines in a hydrophobic environment to direct oxidative protein folding in the mitochondria. Nat. Commun. *5*, 3041.

Li, X., Zhao, X., Fang, Y., Jiang, X., Duong, T., Fan, C., Huang, C.C., and Kain, S.R. (1998). Generation of destabilized green fluorescent protein as a transcription reporter. J. Biol. Chem. *273*, 34970–34975.

Maté, M.J., Ortiz-Lombardía, M., Boitel, B., Haouz, A., Tello, D., Susin, S.A., Penninger, J., Kroemer, G., and Alzari, P.M. (2002). The crystal structure of the mouse apoptosis-inducing factor AIF. Nat. Struct. Biol. *9*, 442–446.

Milenkovic, D., Ramming, T., Müller, J.M., Wenz, L.S., Gebert, N., Schulze-Specking, A., Stojanovski, D., Rospert, S., and Chacinska, A. (2009). Identification of the signal directing Tim9 and Tim10 into the intermembrane space of mitochondria. Mol. Biol. Cell *20*, 2530–2539.

Murray, P., and Edgar, D. (2001). The regulation of embryonic stem cell differentiation by leukaemia inhibitory factor (LIF). Differentiation *68*, 227–234.

Naoé, M., Ohwa, Y., Ishikawa, D., Ohshima, C., Nishikawa, S., Yamamoto, H., and Endo, T. (2004). Identification of Tim40 that mediates protein sorting to the mitochondrial intermembrane space. J. Biol. Chem. *279*, 47815–47821.

Norberg, E., Karlsson, M., Korenovska, O., Szydlowski, S., Silberberg, G., Uhlén, P., Orrenius, S., and Zhivotovsky, B. (2010). Critical role for hyperpolarization-activated cyclic nucleotide-gated channel 2 in the AIF-mediated apoptosis. EMBO J. *29*, 3869–3878.

Otera, H., Ohsakaya, S., Nagaura, Z., Ishihara, N., and Mihara, K. (2005). Export of mitochondrial AIF in response to proapoptotic stimuli depends on processing at the intermembrane space. EMBO J. *24*, 1375–1386.

Parrish, J.Z., and Xue, D. (2003). Functional genomic analysis of apoptotic DNA degradation in C. elegans. Mol. Cell *11*, 987–996.

Pfanner, N., van der Laan, M., Amati, P., Capaldi, R.A., Caudy, A.A., Chacinska, A., Darshi, M., Deckers, M., Hoppins, S., Icho, T., et al. (2014). Uniform nomenclature for the mitochondrial contact site and cristae organizing system. J. Cell Biol. *204*, 1083–1086.

Pospisilik, J.A., Knauf, C., Joza, N., Benit, P., Orthofer, M., Cani, P.D., Ebersberger, I., Nakashima, T., Sarao, R., Neely, G., et al. (2007). Targeted deletion of AIF decreases mitochondrial oxidative phosphorylation and protects from obesity and diabetes. Cell *131*, 476–491.

Qi, Y., Tian, X., Liu, J., Han, Y., Graham, A.M., Simon, M.C., Penninger, J.M., Carmeliet, P., and Li, S. (2012). Bnip3 and AIF cooperate to induce apoptosis and cavitation during epithelial morphogenesis. J. Cell Biol. *198*, 103–114.

Rinaldi, C., Grunseich, C., Sevrioukova, I.F., Schindler, A., Horkayne-Szakaly, I., Lamperti, C., Landouré, G., Kennerson, M.L., Burnett, B.G., Bönnemann, C., et al. (2012). Cowchock syndrome is associated with a mutation in apoptosis-inducing factor. Am. J. Hum. Genet. *91*, 1095–1102.

Sideris, D.P., Petrakis, N., Katrakili, N., Mikropoulou, D., Gallo, A., Ciofi-Baffoni, S., Banci, L., Bertini, I., and Tokatlidis, K. (2009). A novel intermembrane space-targeting signal docks cysteines onto Mia40 during mitochondrial oxidative folding. J. Cell Biol. *187*, 1007–1022.

Susin, S.A., Lorenzo, H.K., Zamzami, N., Marzo, I., Snow, B.E., Brothers, G.M., Mangion, J., Jacotot, E., Costantini, P., Loeffler, M., et al. (1999). Molecular characterization of mitochondrial apoptosis-inducing factor. Nature *397*, 441–446.

Szklarczyk, R., Wanschers, B.F., Nabuurs, S.B., Nouws, J., Nijtmans, L.G., and Huynen, M.A. (2011). NDUFB7 and NDUFA8 are located at the intermembrane surface of complex I. FEBS Lett. *585*, 737–743.

Vahsen, N., Candé, C., Brière, J.J., Bénit, P., Joza, N., Larochette, N., Mastroberardino, P.G., Pequignot, M.O., Casares, N., Lazar, V., et al. (2004). AIF deficiency compromises oxidative phosphorylation. EMBO J. *23*, 4679–4689.

Weis, B.L., Schleiff, E., and Zerges, W. (2013). Protein targeting to subcellular organelles via MRNA localization. Biochim. Biophys. Acta *1833*, 260–273.

Yang, J., Staples, O., Thomas, L.W., Briston, T., Robson, M., Poon, E., Simões, M.L., El-Emir, E., Buffa, F.M., Ahmed, A., et al. (2012). Human CHCHD4 mitochondrial proteins regulate cellular oxygen consumption rate and metabolism and provide a critical role in hypoxia signaling and tumor progression. J. Clin. Invest. *122*, 600–611.

Ye, H., Cande, C., Stephanou, N.C., Jiang, S., Gurbuxani, S., Larochette, N., Daugas, E., Garrido, C., Kroemer, G., and Wu, H. (2002). DNA binding is required for the apoptogenic action of apoptosis inducing factor. Nat. Struct. Biol. *9*, 680–684.